Thiophene and Pyrrole Derivative Polymers Electro-Synthesized on Stainles Steel. Doping and Morphology Characterization

G. C. Arteaga [1], M. A. del Valle[1,*], M. Antilén [1], F. R. Díaz [1], M. A. Gacitúa [1], P. P. Zamora [1], J. C. Bernède [2], L. Cattin [3], and G. Louarn [3]

[1] Pontificia Universidad Católica de Chile, Facultad de Química, Departamento de Química Inorgánica, Laboratorio de Electroquímica de Polímeros (LEP), Vicuña Mackenna 4860, 7820436, Macul, Santiago, Chile.
[2] Université de Nantes, MOLTECH-Anjou, CNRS, UMR 6200, 2 rue de la Houssinière, BP 92208, Nantes, F-44000 France.
[3] Université de Nantes, Institut de Materiux Jean Rousel (IMN), CNRS, UMR 6205, 2 rue de la Houssinière, BP 32229, 44322, Nantes Cedex 3 France.
[*]E-mail: mdvalle@uc.cl

3,4-ethylenedioxythiophene (EDOT), 3,4-propylenedioxythiophene (PRODOT), 3,4-ethylenedioxypyrrole (PEDOP) and 3,4 propylenedioxypyrrole (PRODOP), thiophene and pyrrole derivatives, were electro-polymerized by potentiodynamic and potentiostatic methods on stainless steel AISI 316 electrodes, using lithium perchlorate as support electrolyte in acetonitrile. In all cases electrodes modified with the respective polymeric deposit (PEDOT, PPRODOT, PPEDOP and PPRODOP) were obtained. One of the most relevant features of these polymers is that their voltammetric responses revealed that all presented $p-$ and $n-doping/undoping$ processes, being both processes reversible. Moreover, nucleation and growth mechanism (NGM) of the polymers was established by deconvolution of the experimental j/t transients recorded during it electropolymerization. PEDOT and PPRODOP showed a single contribution to the overall process, corresponding to instant nucleation with three-dimensional growth, controlled by charge transfer, whereas pyrrole derivatives (PEDOP and PPRODOP) are controlled by the same contribution, but there is also a second one corresponding to progressive nucleation with diffusion-controlled three-dimensional growth. Nuclei shape predicted from these NGM is consistent with the respective morphologies determined by SEM and AFM that, once more, validated the proposed electropolymerization model and the morphology prediction from the NGM of the respective polymers. To sum up, a correlation between the structure of the starting unit, *doping*, and morphology of the electro-deposited polymers was established.

1. INTRODUCTION

The electro-synthesis of polymers from pyrrole and thiophene derivatives, *e.g.* 3,4-ethylenedioxythiophene, EDOT, has been thoroughly studied on various electrode materials, especially considering the potential use of its polymer, PEDOT, in applications such as photocells, light emitting diodes, batteries, fuel cells, sensors, etc. [1-12]. An important property of these polymers is their ability to be doped *via* partial oxidation or reduction. The use of electrochemical techniques offer, again, advantages here because the *doping/undoping* occur simultaneously during the synthesis, or else, may be subsequently modulated in a controlled manner. Thus, in the case of partial oxidation, p-type *doping* or p-*doping* takes place. This process generates a positively charged polymer, which entails the entry of counter-anions. On the other hand, when partial reduction of the polymeric film occurs, negative charges will be generated and therefore countercations are incorporated. This process is called n-type *doping* or n-*doping* [13,14]. p-*doping* has been widely studied, while the n-*doping* was first mentioned only in 1994 [15] and since then, only a few publications have addressed the issue [16-19], emphasizing that the stability of n-doped conductive polymers enables their application in microelectronic devices [20].

By contrast, PEDOT homologs, such as polymers to be obtained from 3,4-propylenedioxythiophene (PRODOT), 3,4-ethylenedioxypyrrrole (PEDOP) or 3,4 propylene dioxypyrrole (PRODOP) have been very little explored, although they should be useful to predict or explain the behavior of this kind of materials. This is one of the major weaknesses in this area, wherein light emitting diodes, batteries, fuel cells, super-capacitors, sensors and biosensors of these polymers have been developed on different electrode substrates [21-27]. It has also been stressed that, among the aforementioned polymers, PEDOT has been reported to have the highest *doping* levels when different supporting electrolytes are employed [28,29], while, apparently, the rest presented lower levels [23,30].

Therefore, the goal of the current work is an attempt to correlate monomer structure with the morphology and topology that can present the electro-generated polymers deposited on a steel AISI type 316 electrode, starting from the abovementioned monomers, whose structural formulas are illustrated in Scheme 1.
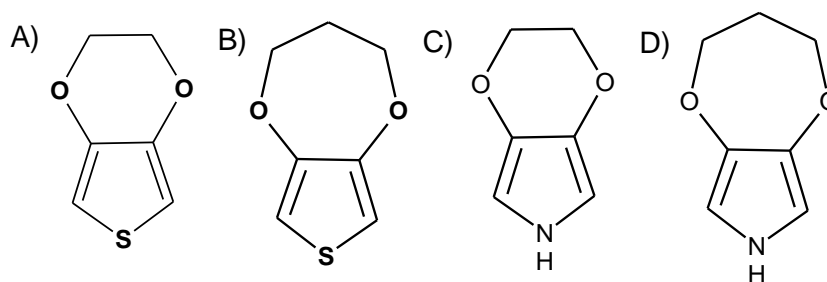
Scheme1. A) EDOT; B) PRODOT; C) EDOP; D) PRODOP.

It is relevant to perform the electro-polymerization and characterization of these pyrrole and thiophene derivatives, focusing primarily on p- and n-type *doping* and *undoping* properties that could

define their prospective applications. Deposits will be obtained on steel; the low cost of this electrode material would allow speculating on future applications. At the same time, depending on its desired use, a systematic study will be conducted aimed at finding the optimal starting unit.

The electrochemical synthesis allows for *in situ* characterization using potentiodynamic (cyclic voltammetry) and potentiostatic techniques that will establish the *doping/undoping* processes and the nucleation and growth mechanisms (NGM), respectively. The latter will be correlated with the morphological characterization results, to be carried out by scanning electronic (SEM) and atomic force (AFM) microscopy, to corroborate if the NGM enables morphology prediction as established in other cases [31-38]. Besides, a morphology correlation with starting unit structure and with their macroscopic properties, *e.g.* conductivity and type of doping, will be searched for.

2. EXPERIMENTAL

All aqueous solutions were prepared with freshly deionized water in a Heal Force (Smart Series) deionizer. All measurements were performed at room temperature (20 °C) under high purity argon atmosphere in anchor-type three-compartment electrochemical cells. The working electrode was a 0.07 cm^2 geometric area AISI 316 stainless steel disc. The counter electrode was a platinum wire coil of large geometric area. Ag/AgCl in tetramethylammonium chloride solution, its potential adjusted to a saturated calomel electrode, SCE, was utilized as reference electrode [39]. Unless otherwise stated, all potentials quoted in the current work are referred to this electrode at room temperature.

EDOT (97%, Aldrich), PRODOT (97%, Aldrich), EDOP (2% w/v in tetrahydrofuran (THF), Aldrich) and PRODOP (2% w/v in THF, Aldrich) electro-oxidation was optimized to obtain the respective polymeric deposits, *i.e.* PEDOT, PPRODOT, PEDOP and PPRODOP using the aforementioned steel electrode, cell assembly and working conditions.

Polymers synthesis was conducted using cyclic voltammetry, CV, at 50 or 100 mV s^{-1} scan rate, and within various potential windows. Solutions having different monomer concentration and various supporting electrolytes were employed.

Thus, after numerous attempts, the optimal working conditions that permits working with all the four starting unit proposed herein, were as follows. Monomer concentration 0.01 mol L^{-1}; supporting electrolyte 0.1 mol L^{-1} lithium perchlorate (LiClO$_4$ 99%, Aldrich) in acetonitrile (CH$_3$CN 99.8%, Aldrich), the latter being suitable for working with the four monomers in the following potential windows: -1.0 to 1.5 V (EDOT) -1.0 to 1.6 V (PRODOT) -1.0 to 2.0 V (EDOP) and -1.0 to 1.9 V (PRODOP).

From these results, the potentiostatic method (PM) was attempted. It was established that the more appropriate fixed potential to be imposed to prepare the modified electrodes was 1.40, 1.58, 2.00 and 1.80 V for PEDOT (SS/PEDOT), PPRODOT (SS/PPRODOT), PEDOP (SS/PEDOP), and PPRODOP (SS/PPRODOP), respectively.

In each example, to optimize the conditions to be employed, the stable electrochemical response of the modified electrode in supporting electrolyte solution was determined. This enabled the

respective p-*doping/undoping* and n-*doping/undoping* processes to be analyzed in order to find the amount of charge involved and, chiefly, the most reversible response.

All electrochemical measurements (polymerization and characterization) were performed on an AUTOLAB PGSAT 20 potentiostat. Morphology of deposited polymers was analyzed by scanning electron microscopy (SEM) on a JEOL 6400 F microscope. Morphology and topography details of these polymers were examined by atomic force microscopy on a BIO AFM JPK microscope.

3. RESULTS AND DISCUSSION

Figure 1 illustrates monomers voltammetric profile for their electrochemical oxidation during potentiodynamic successive cycles, under the experimental conditions (concentration, supporting electrolyte) and within the working range set forth herein as optimal. The increase of current between successive cycles is an evidence of polymer growth, as well as a clear indication that p- and n-*doping* processes occur. It can also be seen that EDOT (Fig. 1B) presents a greater amount of current and charge than the other electro-polymerized monomers. PRODOP, owing to poor adhesion to the electrode surface, was the sole monomer that exhibited no reproducible results by potentiodynamic electro-polymerization, and its voltammetric profile was not included in Fig.1. However, as will be shown below, this was achieved by using the potentiostatic approach.
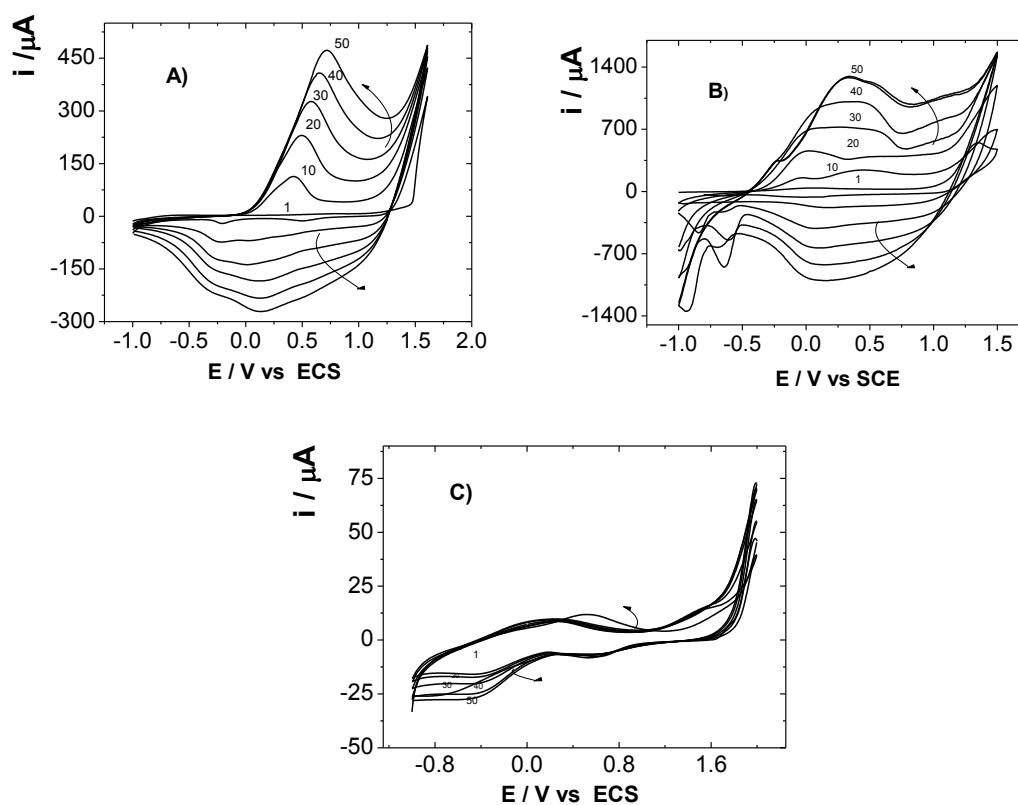
Figure 1. Monomer voltammetric profiles. Interfaces: SS/0.01 mol L^{-1} monomer + 0.1 mol L^{-1} LiClO$_4$, CH$_3$CN. $\nu = 50$ mV s^{-1}. A) PRODOT; B) EDOT; C) EDOP.

Figure 2 shows the voltammetric response in the n-*doping-undoping* potential range of modified electrodes with polymeric electro-deposits obtained by CV under the optimum condition established herein (SS/PEDOT, SS/PPRODOT and SS/PEDOP). As for SS/PPRODOP, the response corresponds to the deposit synthesized by the potentiostatic method. As can be seen, the response in solutions containing just supporting electrolyte (LiClO$_4$), effectively revealed the existence of n-*doping/undoping* processes that allow designing the use of these polymeric deposits in applications wherein this property is crucial, *e.g.* cation exchange [40, 49-53].
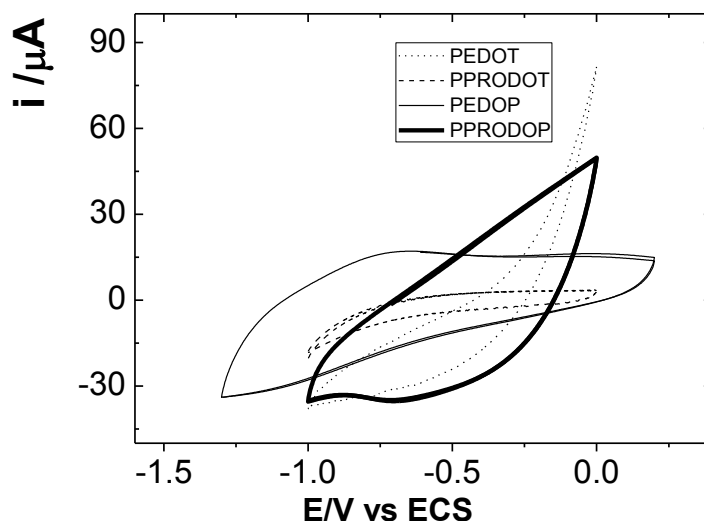
Figure 2. Response in the n-*doping/undoping* potential region of SS electrodes modified by polymeric deposits indicated in the insert.

Table 1 summarizes the respective negative (E$_{cat}$) and positive (E$_{an}$) limits wherein this phenomenon occurs for each studied polymer and the respective n-*doping/undoping,* charge. The results revealed these processes are totally reversible, since the ratio between the charges obtained from the electrochemical responses (Fig. 2) are practically unit. Nevertheless, the reversibility order is PEDOP> PPRODOP> PEDOT> PPRODOT, which can be attributed to the conformation of the polymer matrix of each one that is determined, on the one hand, by the heteroatom and, on the other, by the length of the alkyl chain between oxygen atoms. Computational calculations and molecular dynamics studies are proposed to corroborate these results and establish a more stringent correlation between structure of the starting unit and polymeric matrix.

Figure 3 displays the p-*doping/undoping* processes of the same polymeric deposits, in the potential range summarized in Table 2, along with the respective charges. It can be seen that charge ratios are close to one, which means the processes are reversible with respect to charge or p-*doping/undoping* level. Nonetheless, from Fig. 3 responses, the order of reversibility is PEDOT> PPRODOT> PEDOP> PPRODOP that differs from that found for n-*doping/undoping* processes (Fig. 2 and Table 1). This can be ascribed to EDOT oxidation potential or to the polymerization potential of this monomer that, as shown in Table 3, presents the lowest value of all the starting units surveyed.

Table 1. n-*doping* (n-Q_d) and n-*undoping* (n-Q_u) charge of electrosynthesized polymers on SS within the respective negative (E_{cat}) and positive (E_{an}) potential limits.

Polymer	E_{cat} (V)	E_{an} (V)	n-Q_d (C)	n-Q_u (C)	n-Q_d:n-Q_d (C)
PEDOT	-1.0	0.0	$7.94 \cdot 10^{-5}$	$8.50 \cdot 10^{-5}$	0.98
PPRODOT	-1.0	0.0	$1.84 \cdot 10^{-5}$	$1.65 \cdot 10^{-5}$	1.11
PEDOP	-1.3	0.3	$3.48 \cdot 10^{-4}$	$3.46 \cdot 10^{-4}$	0.99
PPRODOP*	-1.0	0.0	$2.92 \cdot 10^{-4}$	$2.91 \cdot 10^{-4}$	1.03

* Polymer electro-synthesized by potentiostatic method, as detailed below

However, it is noteworthy that always the respective charge of the p-*doping* process is greater than that of the n-*doping*. This phenomenon has been corroborated in previous studies [40-43] and is explained considering it is easier for a polymeric matrix to give up electrons, *i.e.* to become positively charged *(p-doping),* than take up electrons (n-*doping)*. The latter issue is reflected in the charge found for each of the electrochemical responses illustrated in Figs. 2 and 3.
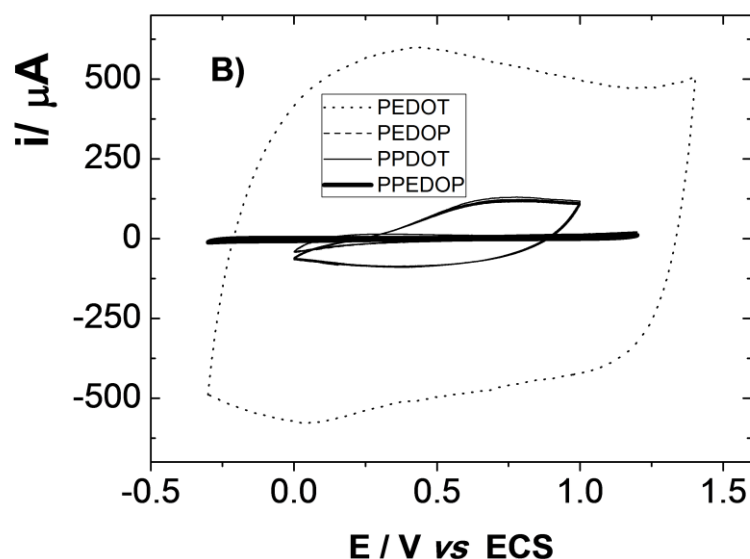
Figure 3. Response in the p-*doping-undoping* potential range of SS electrodes modified by the deposits indicated in the insert.

The optimal conditions, established by voltammetric characterization, were utilized to conduct potential controlled electro-polymerization. The same steel electrodes were employed in solutions similar to those already described as optimum, at a potential close to the anodic switching potential of each monomer. Figure 4 shows examples of the j/t obtained transients that enabled determining, in each case, the optimum potential to be applied in this particular technique. If the potential were much higher than the optimal one, the deposit would foul up by over-oxidation and its reproducibility would

be totally lost while at lower potentials, electrolysis would take very long times or it definitely would not occur.

Table 2. p-*doping* (p-Q_d) and p-*undoping* (p-Q_u) charge of polymers synthesized at SS electrodes within the respective limits of negative (E_{cat}) and positive (E_{an}) potential.

Polymer	E_{cat} (V)	E_{an} (V)	n-Q_d (C)	n-Q_u (C)	n-Q_d:n-Q_d (C)
PEDOT	0.3	1.4	$1.50 \cdot 10^{-2}$	$1.47 \cdot 10^{-2}$	1.20
PPRODOT	0.0	1.0	$6.24 \cdot 10^{-4}$	$5.52 \cdot 10^{-4}$	1.31
PEDOP	0.0	1.1	$1.22 \cdot 10^{-4}$	$1.10 \cdot 10^{-4}$	1.10
PPRODOP*	0.3	1.2	$2.44 \cdot 10^{-4}$	$2.58 \cdot 10^{-4}$	0.98

* Polymer electro-synthesized by potentiostatic method, as detailed below
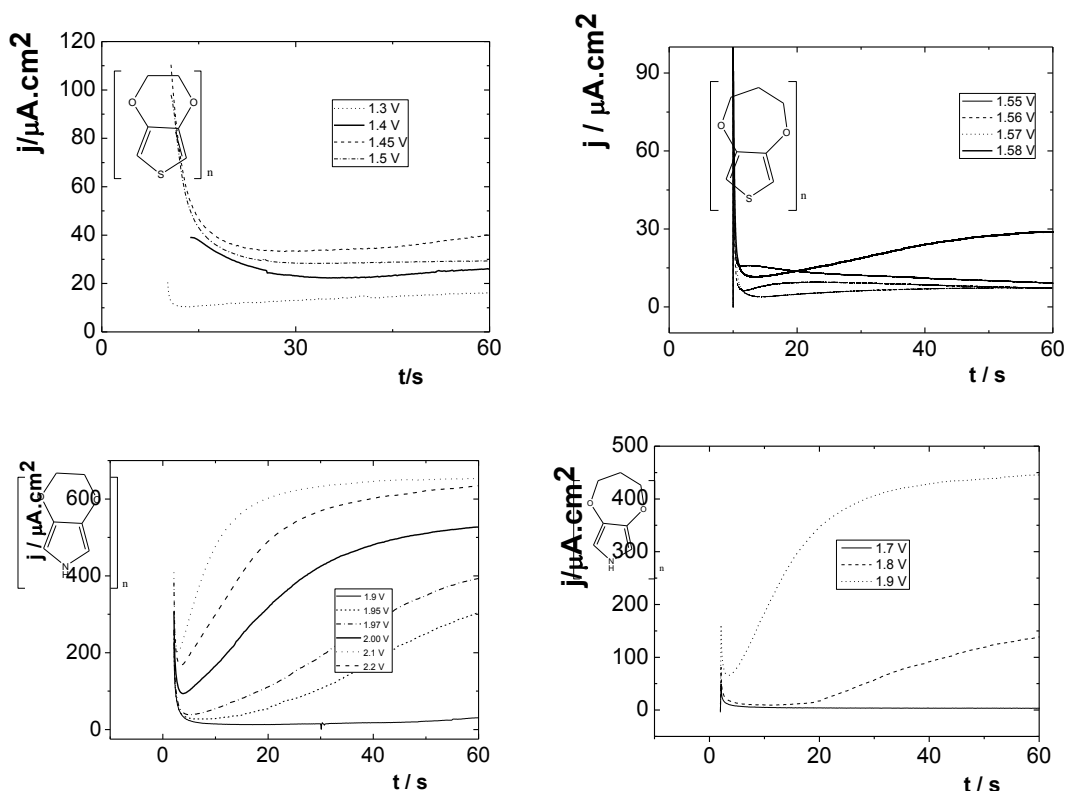
Figure 4. j/t transients recorded during potentiostatic monomers electro-polymerization. (E and monomer are those indicated in the inset). Interface: SS/0.01 EDOT + 0.1 mol L^{-1} LiClO$_4$, CH$_3$CN.

The j/t transients shown as example in Fig. 3 revealed that when working at controlled potential in the nucleation and growth region, a general pattern of behavior exists that can be described considering, first, that after the initial current rise and exponential decay, attributable to monomer oxidation, the current increases again as nucleation takes place, giving rise to deposit growth (induction time, τ, depending on such growth [31, 43 - 50].

Thus, it can be observed for each case that at potentials lower than the optimum, the induction time, τ, is very high, while at higher potentials is very low and erratic, with total reproducibility loss, *i.e.* over-oxidation of the generated coating occurs. On this basis, the most suitable potential for each of the studied monomers, when potentiostatic deposition is the technique of choice, are depicted in Table 3. The electro-oxidation potential order to conduct the potentiostatic electro-polymerization on SS, from highest to lowest, was PEDOP> PPRODOP> PPRODOT> PEDOT.

Table 3. Optimum potential for the electrosynthesis of each polymer, to prepare SS modified electrodes by PM, from solutions similar to those of Fig.1.

Polymer	E_{ox} (V)
PEDOP	2.00
PPRODOP	1.80
PPRODOT	1.58
PEDOT	1.40

This and the rest of trends regarding current and potential values are explained, as aforementioned, from monomer structure. The latter correlates with the heteroatom and length of the alkyl chain between oxygen atoms. This assumption will be confirmed by theoretical calculations. Meanwhile, this oxidation potential trend can be interpreted by means of the monomeric structure (Scheme 1), wherein pyrrole derivatives possess nitrogen in their structure, unlike thiophene derivatives that contain sulfur. According to valence bond theory, sulfur bears two lone non-bonding pairs of electrons, of which only one pair is in the unhybridized p-orbital and can overlap with carbon atoms of the ring in its structure. This feature increases the resonance (stability) of the oligomeric structures formed during the early stages of electropolymerization and hence their formation is favored. Consequently, the oxidation potentials required for the electro-oxidation of thiophene derivatives (PEDOT and PPRODOT) are lower than those of pyrrole (PEDOP and PPRODOP) derivatives, whose heteroatom is nitrogen that presents sp^2 hybridization, with a lone pair of electrons in the p-orbital. This orbital overlaps the p-orbital of the carbon atoms to form molecular orbitals that increase electron delocalization, *i.e.* the starting unit being more stable in this case. Hence, both pyrrole derivatives have a higher oxidation potential as compared to those of the respective thiophene analogue derivatives.

Figure 4 shows deconvolution of the respective time-current transients recorded during the controlled potential electropolymerization from the monomers under the optimal conditions established herein. With the obtained data, as previously described for similar studies [35, 37.50 - 54], the respective NGM were determined.
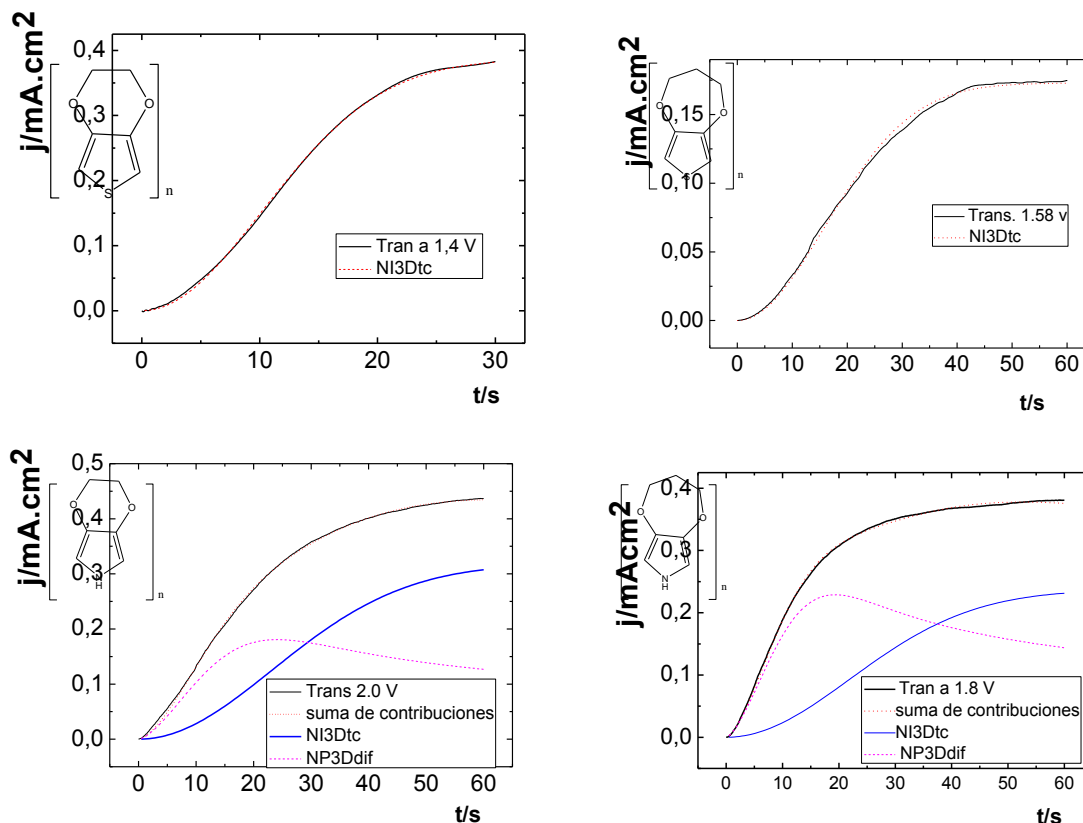
Figure 5. Deconvolution of current-time transients recorded on SS, under the optimum conditions and using the potential listed in Table 3 (the respective curve and monomer are indicated in the inset).

The equations that describe the contributions that enabled the obtained transients to be deconvoluted, and that correspond to the respective NGM, are as follows: charge transfer controlled 3D instantaneous nucleation (IN3D$_{tc}$) and 3D progressive nucleation with diffusion-controlled growth (PN3D$_{diff}$) [55]:

$$i = P_1\left[1 - e^{-P_2 t^2}\right] \qquad (1)$$

$$i = t^{-1/2} P_3\left[1 - e^{-P_4 t^2}\right] \qquad (2)$$

It is noteworthy that these results are in agreement with those previously reported for PEDOT NGM when working on platinum and fluorine-doped tin oxide because the same contributions were found, *i.e.* the same mechanism exists [47].

As shown in Figs. 5 A) and 5 B) PEDOT and PPRODOT require a single contribution to deconvolve the whole transient, *i.e.*, the NGM would be made up of a single process, IN3D$_{tc,}$ which accounts for the formation of a determined number of nuclei that will grow simultaneously as circular based cones.

On the other hand, in PPRODOP and PEDOP, as seen in Figs. 5C) and 5D), the respective global NGM responds to the sum of two contributions, although one of them is the same as above, *i.e.*

a certain number of cones with a circular base, of uniform size, would exist as well. Besides, there would be a PN3D$_{dif,}$ contribution that accounts for the semi-spheres that appear and grow as a function of electrolysis time [40-44].

The parameters of equations (1) and (2) are displayed in Table 4, where F is the Faraday constant, n number of electrons involved, monomer *M* molar mass, ρ film density, k$_{3D}$ 3D growth parallel to the electrode rate constant, A$_{3D}$ nucleation rate constant, and D diffusion coefficient. A$_{diff}$ and N$_{diff}$ are nucleation rate constants in the steady state and diffusion-controlled number formed nuclei, respectively [41.50]. P$_1$, P$_2$, P$_3$ and P$_4$ values obtained by transient deconvolution (Fig. 5), that allowed accurate simulation of the experimental transients, are summarized in Table 5.

Table 4. Expressions for parameters of equations (1) and (2).

Parameter	Expression
P$_1$	nFk_{3D}
P$_2$	$\dfrac{\pi N_{3D} A_{3D} M^2 k_{3D}^2}{3\rho^2}$
P$_3$	$\dfrac{SnFC\sqrt{D}}{\sqrt{\pi}}$
P$_4$	$\dfrac{2\pi D A_{dif} N_{dif}}{3}\left(\dfrac{8\pi CM}{\rho}\right)^{1/2}$

Values in Table 5 highlight, first, that r^2 close to 1 indicates a clear correlation between the experimental and simulated transients, consequently the obtained NGM would be reliable. Second, the P parameters showed a correlation with the monomer structure and are consistent with the proposed electro-polymerization model. As shown in Fig. 5 the profiles obtained by deconvolution or addition of the curves calculated from the respective deconvolution equations (using Table 5 constants), almost exactly coincide with the experimentally attained transients.

Subsequently, to determine the morphology of the deposits and, particularly, to validate the simulations leading to the obtention of the different NGM of each of the described polymers, SEM characterization was performed, Fig. 6. Micrographs in Fig. 6 revealed that the morphology of each deposit corroborates the previously proposed models: Figs. 6A) and 6B) show that the grown nuclei are quite uniform and of homogenous form, although in 6A) the growth was faster than in 6B), as may be inferred from the respective j/t transients and NGM established from their deconvolution. In both cases only one type of nuclei, formed at the same time, exist and therefore are similar to each other in size, although the deposit in 6A) has grown more than in 6B), which is consistent with the higher currents recorded.

Table 5. Numerical values of the parameters of equations (1) and (2), described in Table 4, suitable for transient deconvolution j/t recorded on SS (Fig.4).

[Polymer] (mol·L^{-1})	E (V)	P$_1$ (µA·cm^2)	P$_2$ (ms^{-2})	P$_3$ (mA·cm^{-2}·s$^{1/2}$)	P$_4$ (ms^{-2})	r^2
PEDOT	1.40	24.70	22.10	-	-	0.9965
PPRODOT	1.58	17.30	19.80	-	-	0.9943
PEDOP	2.00	31.90	10.20	0.98	0.42	0.9996
PPRODOP	1.80	23.70	10.40	1.11	0.62	0.9993

In contrast, Fig. 6 C) shows that a difference exists among nuclei, as semi-spheres of different sizes can be observed, which agrees with a progressive nucleation mechanism. It must be emphasized, however, that in the case of PPRODOP it proved impossible to perform SEM analysis, since very thin films were produced, making unfeasible the obtention of suitable amounts of deposit necessary for conducting this type of characterization.

To corroborate the morphology predicted from the NGM, AFM technique was also utilized. The results are summarized in Fig. 7 and are remarkable, since the morphologies clear and exactly agree with those predicted from the NGM. The first two, corresponding to PEDOT and PPRODOT, exhibit similar morphology, *i.e.* both display the same mechanism and present just one contribution to the NGM that justifies the formation of a more homogeneous deposit.

A

B

C
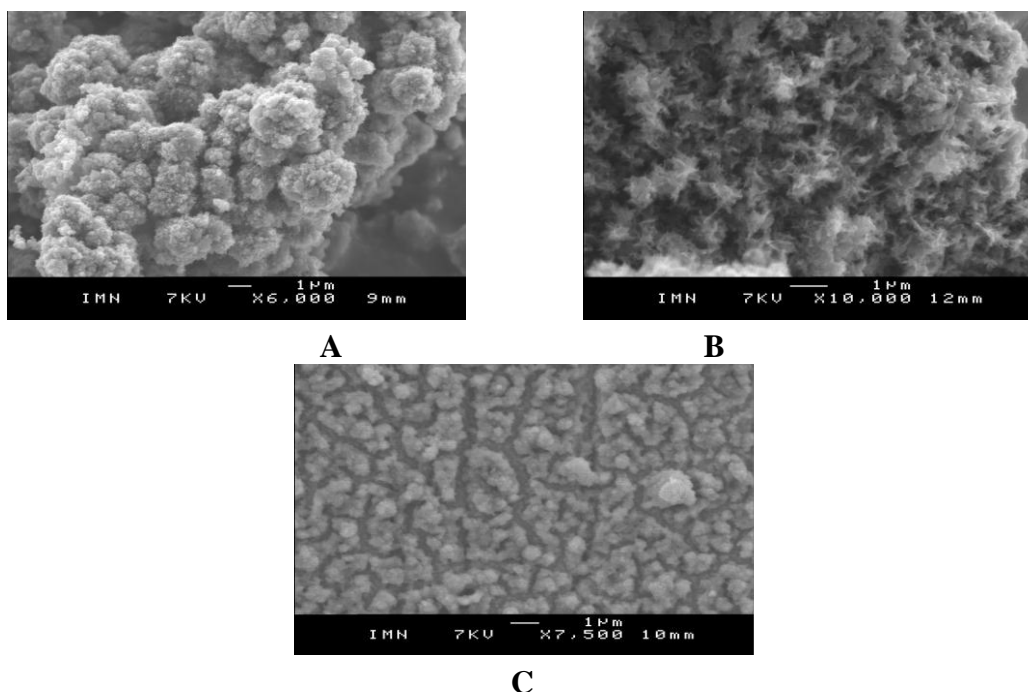
Figura 6. Deposits: A) PEDOT, B) PPRODOT, C) PEDOP on SS, 30 min after the induction time ▢.

PEDOP's NGM involves two contributions, consistent with the morphology that exhibits two types of nuclei, growing at different rates, affording thus a more heterogeneous surface.
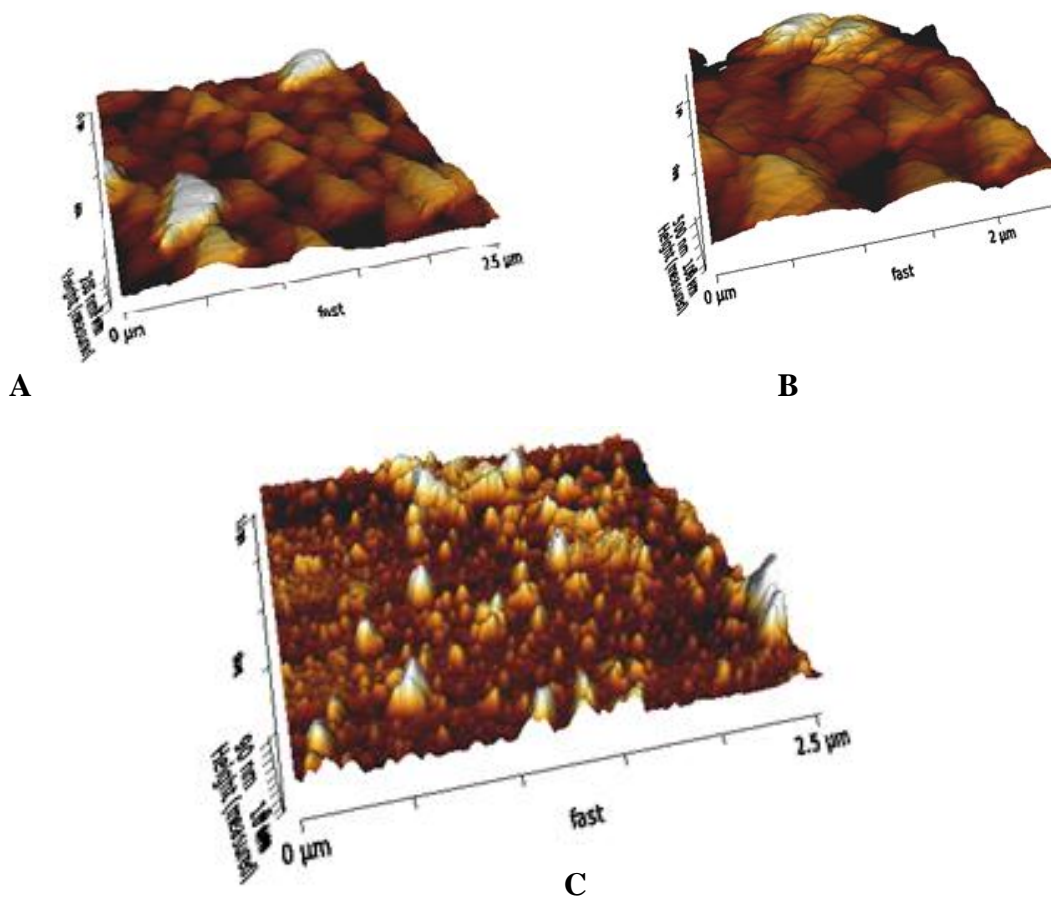
Figure 7. A) PEDOT, B) PPRODOT and C) PEDOP deposition on SS, 1 min after induction time.

Finally, as aforementioned, a correlation between the structure of the monomer with the morphology and macroscopic properties of these polymeric electro-deposits will be searched for. In this case, EDOP is the monomer that generates a polymeric deposit with the highest n-*doping/undoping* charge. This can be justified by its morphology that is less uniform and much more porous than the other deposits, allowing more and better cation exchange. Consequently, among all modified electrodes prepared, PEDOP would be the most suitable for use, for example, in cation removal.

Therefore, considering the previously reported process for mercuric ion extraction or removal [36], a comparison of the electrochemical response was made in the n-*doping/undoping* region of the different modified electrodes prepared at the optimum conditions established here. Using Hg(II)-containing phosphate buffer at physiological pH, PBS, it was verified that also for this ion SS/PPRODOP presented the greatest reversibility (Fig. 8 and Table 6).
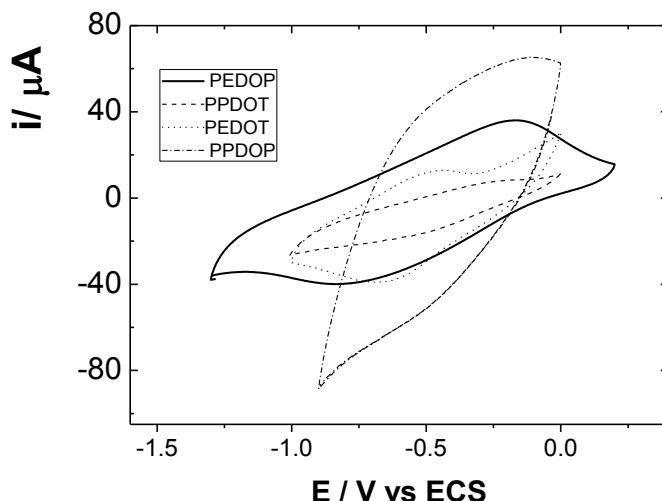
Figure 8. Response in Hg(II) solutions at physiological pH. Perturbation at the n-*doping/undoping* potential region of deposits shown in the insert, on SS.

Table 6. Charges of n-*doping* (n-Qd) and n-*undoping* (n-Qu) of electro-synthesized polymers under identical conditions, on SS within the respective negative (E_{cat}) and positive limits (E_{an}).

Polymer	E_{cat} (V)	E_{an} (V)	n-Q_d (C)	n-Q_u (C)	n-Q_d:n-Q_d (C)
PEDOT	-1.0	0.0	$4.0 \cdot 10^{-4}$	$4.0 \cdot 10^{-4}$	1.0
PPRODOT	-1.0	0.0	$1.4 \cdot 10^{-4}$	$1.8 \cdot 10^{-4}$	0.8
PEDOP	-1.3	0.2	$4.4 \cdot 10^{-4}$	$4.4 \cdot 10^{-4}$	1.0
PPRODOP*	-0.9	0.0	$6.0 \cdot 10^{-4}$	$6.0 \cdot 10^{-4}$	1.0

Based on these results, optimization of the mentioned extraction process is proposed, using the PEDOP modified electrode, as it should display a greater efficiency than that reported for SS/PEDOT, because its response, in the same solution, gives up twice the charge and, in addition, is more reversible.

Finally, studies are performed by computer calculations and molecular dynamics to establish more rigorous correlations between the structure of the starting unit and properties of the respective electro-deposit herein established.

4. CONCLUSIONS

Polymeric deposits of pyrrole and thiophene derivatives were obtained on stainless steel. Both derivatives exhibited n- and p-*doping/undoping* processes. Although the thiophene derivatives charging process showed always greater charge than the pyrrole derivatives, both are practically reversible in regard to the respective charges involved.

Besides of p- and n-*doping/undoping* processes characterization, which allows proposing and choosing the most adequate starting unit in terms of the use to be given to the polymeric deposit,

experimental transients of thiophene and pyrrole derivatives were simulated. The results revealed that both derivatives had an $IN3D_{tc}$ contribution, but, in addition, pyrrole derivatives also presented a $PN3D_{diff}$, contribution. A correlation coefficient, r^2, of approximately 1 for all simulations and the fact that the morphology associated to these NGM correlates exactly with the experimentally determined by SEM and AFM is noteworthy too.

This way, once more the previously proposed electropolymerization model was validated and it was demonstrated that is possible to establish a correlation amidst starting unit structure, *doping*, and polymeric coating morphology.

References

1. H. Hoppe, and N. Sariciftci, *J. Mater. Res.,* 19 (2004) 1924.
2. D. McGehee, and M. Topinka, *Nat. Mater.,* 5 (2006) 675.
3. T. Hebner, C. Wu, D. Marcy, M. Lu, and J. Sturm, *Appl. Phys. Lett.,* 72 (1998) 519.
4. B. Jayesh, and Y. Yang, *Appl. Phys. Lett.,* 72 (1998) 2660.
5. H. S. Nalwa, *Handbook of Nanostructured Materials and Nanotechnology*, Ed. Academy Express, San Diego (2000).
6. R. Schrebler, P. Grez, P. Cury, C. Veas, M. Merino, H. Gómez, R. Córdova, and M. A. del Valle, *J. Electroanal. Chem.,* 430 (1997) 77.
7. M. A. del Valle, F. R. Díaz, M. E. Bodini, G. Alonso, G. Soto, and E. Borrego, *Polym. Int.,* 54 (2005) 526.
8. J. P. Soto, F. R. Díaz, M. A. del Valle, C. Núñez, and J. C. Bernède, *Eur. Polym. J.,* 42 (2006) 935.
9. M. A. del Valle, M. Gacitúa, L. I. Canales, and F. R. Díaz. *J. Chil. Chem. Soc.,* 54 (2009) 260.
10. F. Sundfors, H. Gustafsson, A. Ivaska, and C. Kvarnstom, *J. Solid State Elect.,* 14 (2010) 185.
11. C. Ocampo, R. Oliver, E. Armelin, C. Aleman, and F. Estrany, *J. Polym. Res.,* 13 (2006) 193.
12. J. C. Bernède, *J. Chil. Chem. Soc.,* 3 (2008) 1549.
13. Conducting Polymers: Nobel Prize in Chemistry 2000. Current Sci., 79 (2000) 1632.
14. H. Shirakawa, E. Louis, A. G. MacDiarmid, C. K. Chiang, and A. J. Heeger, *J. Chem. Soc. Chem. Comm.*, 285 (1977) 578.
15. Q. Pei, G. Zuccarello, M. Ahlskog, and O. Inganas, *Polymer,* 35 (1994) 1347
16. H. Ahonen, J. Lukkari, and J. Kankare, *Macromol.,* 33 (2000) 6787.
17. C. Aleman, D. Curco, and J. Cassanovas, *Chem. Phys. Lett.,* 23 (2004) 386.
18. C. Kvarnstrom, H. Neugebauer, and A. Ivaska, *J. Mol. Struct.,* 521 (2000) 271.
19. H. Gustafsson, C. Kvarnstrom, and A Ivaska, *Thin Solid Films,* 517 (2008) 474.
20. D. M. de Leeuw, M.M.J. Simenon, A.R. Brown, and R. E. F. Einerhand, *Synth. Met.,* 87 (1997) 53.
21. C. Gaupp, K. Zong, P. Schottland, B. Thompson, C. A. Thomas, and J. Reynolds, *Macromol.,* 33 (2000) 1132.
22. R. M. Walczak, and J. R. Reynolds, *Adv. Mater.*, 18 (2006) 1121.
23. P. Schottland, K. Zong, C. L. Gaupp, B. C. Thompson, C. A. Thomas, I. Giurgiu,R. Hickman, K. A. Abboud, and J. R. Reynolds, *Macromol.,* 33 (2000) 7051.

24. G. Sonmez, I. Schwendeman, P. Schottland, K. Zong, and J. R. Reynolds, *Macromol.,* 36 (2003) 639.
25. E. Unur, J. Ho, J. Roger, J. Mortimer, and J. R. Reynolds, *Chem. Mater*., 20 (2008) 2328.
26. A. S. Sarac, M. Rotman, H. Gilsing, and H. Faltz, *Electrochim. Acta*, 52 (2007) 5856.
27. O. Türkarslan, S. K. Kayahan, and L. Toppare, *Sensor Actuat. B-Chem.,* 136 (2009) 484.
28. W- W. Chiu, J. T. Sejdic , R. P. Cooney, and G. A. Bowmaker, *J. Raman Spectrosc.,* 37 (2006) 1354.
29. S. G. Im, K. K. Gleason, and E. A. Olivetti, *Appl. Phys. Lett*., 90 (2007) 152112.
30. G. Sonmez, I. Schwendeman, P. Schottland, K. Song, and J. Reynolds, *Macromol.*, 36 (2003) 639.
31. M. A. del Valle, G. Soto, L. Guerra, J. Vélez, and F. R. Díaz, *Polym. Bull.,* 51 (2004) 301.
32. R. Schrebler, M.A. del Valle , H. Gómez, C. Veas, and R. Córdova, *J. Electroanal. Chem*., 219 (1995) 380.
33. F. R. Díaz, M. A. del Valle, F. BrovelliL, L. H. Tagle, and J. C. Bernède, *J. Appl. Polym. Sci.,* 89 (2003) 1614.
34. M.A. del Valle, P. Cury, and R. Schrebler, *Electrochim. Acta*, 48 (2002) 397.
35. L. Ugalde, J. C. Bernède, M. A. del Valle, F. R. Díaz, and P. Leray, *J. Appl. Polym. Sci.*, 84 (2002)1799.
36. M. A. del Valle, L. Ugalde, F. R. Díaz, M. E. Bodini, and J. C. Bernède., *J. Appl. Polym. Sci.*, 92 (2004) 1346.
37. M. B. Camarada, P. Jaque, F. R. Díaz, and M. A. del Valle., *J. Polym. Sci. Pol. Phys*., 49 (2011) 1723.
38. G. East, and M. A. del Valle, *J. Chem. Ed.*, 77 (2000) 97.
39. G. C. Arteaga, M. A. del Valle, M. Antilén, M. Faúndez, M. A. Gacitúa, F. R. Díaz, J. C. Bernède, and L. Cattin, *Int. J. Electrochem. Sci*., 6 (2011) 5209.
40. C. Gaupp, K. Zong, P. Schottland, B. Thompson, C. A. Thomas, and J. Reynolds, *Macromol*., 33 (2000) 1132.
41. R. M. Walczak, and J. R. Reynolds, *Adv. Mater*., 18 (2006) 1121.
42. T. Darmanin, and F. Guittard, *J. Am. Chem. Soc*., 131 (2009) 7928.
43. E. Unur, J. Jung, R. Moretimer, and J. R. Reynolds, *Chem. Mater*., 20 (2008) 2328.
44. M. Antilén, and F. Armijo, *J. Appl. Polym. Sci*., 113 (2009) 3619.
45. M. Antilén, M. González, M. Pérez, M. A. Gacitúa, M. A. del Valle, F. Armijo, R. del Río, and G. Ramírez, *Int. J. Electrochem. Sci.,* 6 (2011) 901.
46. M. A. del Valle, G. Soto, L. Guerra, J. Vélez, and F. Díaz, *Polym. Bull.,* 51 (2004) 301.
47. M. A. del Valle, R. A. Santander, F. R. Díaz, M. Faúndez, M. Gacitúa, M. Antilén, and L. A. Hernández, *Int. J. Electrochem. Sci.,* 6 (2011) 6105.
48. H. Gustafsson, C. Kvarnström, and A. Ivaska., *Thin Solid Films*, 517 (2008) 474.
49. H.J. Ahonen, J. Lukkari, and J. Kankare., *Macromol., 33 (2000)* 6787.
50. M. A. del Valle, M. B. Camarada, F. Díaz, and G. East, *e-Polymers*, 72 (2008) 1
51. J. Heinze, B. Frontana-Uribe, and S. Ludwigs, *Chem. Rev.,110 (*2010)4724.
52. R. Córdova, M.A. del Valle, A. Arratia, H. Gómez, and R. Schrebler, *J. Electroanal. Chem.,* 377 (1994) 75.
53. M. A.del Valle, F. R. Díaz, M. E. Bodini, G.Alfonso, G. M. Soto, and E.Borrego, *Polym. Int.*, 54 (2005) 526.
54. M. A. del Valle, M. Gacitúa, E.Borrego, P. Zamora, F. Díaz, M. B. Camarada, M. Antilén, and J. P. Soto, *Int. J. Electrochem. Sci.,* 7 (2012) 2552.
55. E. Horwood, *Instrumental Methods in Electrochemistry;* Southampton Electrochemistry Group, 1985.